Journal of Pharmaceutical Analysis 10 (2020) 78–85

Contents lists available at ScienceDirect

Journal of Pharmaceutical Analysis

journal homepage: www.elsevier.com/locate/jpa

Original Article

Thermodynamics of clay–drug complex dispersions: Isothermal titration calorimetry and high-performance liquid chromatography

Ana-Maria Totea [a], Juan Sabin [b], Irina Dorin [c], Karl Hemming [d], Peter R. Laity [e], Barbara R. Conway [a], Laura Waters [a], Kofi Asare-Addo [a, *]

[a] School of Applied Sciences, Department of Pharmacy, University of Huddersfield, Queensgate, Huddersfield, HD1 3DH, UK
[b] AFFINImeter, Edificio Emprendia, Campus Vida, Santiago de Compostela, Spain
[c] Malvern Panalytical Ltd., Malvern, UK
[d] School of Applied Sciences, Department of Chemistry, University of Huddersfield, Queensgate, Huddersfield, HD1 3DH, UK
[e] Department of Materials Science and Engineering, University of Sheffield, Sir Robert Hadfield Building, Mappin Street, Sheffield, S1 3JD, UK

ARTICLE INFO

Article history:
Received 23 May 2019
Received in revised form
3 December 2019
Accepted 4 December 2019
Available online 5 December 2019

Keywords:
Clay-drug complex dispersions
Magnesium aluminium silicate
Diltiazem hydrochloride
Isothermal titration calorimetry
High performance liquid chromatography

ABSTRACT

An understanding of the thermodynamics of the complexation process utilized in sustaining drug release in clay matrices is of great importance. Several characterisation techniques as well as isothermal calorimetry were utilized in investigating the adsorption process of a model cationic drug (diltiazem hydrochloride, DIL) onto a pharmaceutical clay system (magnesium aluminium silicate, MAS). X-ray powder diffraction (XRPD), attenuated total reflectance Fourier transform infrared spectroscopy (ATR-FTIR) and optical microscopy confirmed the successful formation of the DIL-MAS complexes. Drug quantification from the complexes demonstrated variable behaviour in the differing media used with DIL degrading to desacetyl diltiazem hydrochloride (DC-DIL) in the 2 M HCl media. Here also, the authors report for the first time two binding processes that occurred for DIL and MAS. A competitor binding model was thus proposed and the thermodynamics obtained suggested their binding processes to be enthalpy driven and entropically unfavourable. This information is of great importance for a formulator as care and consideration should be given with appropriate media selection as well as the nature of binding in complexes.

1. Introduction

Minerals have a variety of applications in the pharmaceutical industry and in medicine which date back since prehistory [1]. Minerals have desirable physicochemical properties such as chemical inertness, high adsorption capacity and specific area, swelling, water solubility and dispersivity, plasticity, acid-absorbing capacity, as well as colour, opacity and low or no toxicity in patients, which makes them suitable for medical and pharmaceutical applications [1,2]. In the formulation of pharmaceutical dosage forms, minerals are used as excipients as carriers of active ingredients to achieve modified release, or as binders, fillers, disintegrants, lubricants, thickening agents, anticaking agents, flavouring correctors and emulsifying agents [2].

Magnesium aluminium silicate (MAS or *VEEGUM®*) is a mixture of natural smectite montmorillonite and saponite clays (Fig. 1). MAS has a layered silicate structure, formed of one alumina or magnesia octahedral sheet, sandwiched between two tetrahedral silicate sheets [3,4]. The high surface area and good affinity with cationic drugs, as well as its non-toxic properties make MAS a suitable material for use in drug formulation. MAS has previously been shown to be able to adsorb cationic drugs such as propranolol hydrochloride and form complexes that are able to retard drug release [5–7]. Controlling drug release is of high interest as it has been demonstrated to show many benefits compared with conventional drug release. By maintaining a constant drug-plasma concentration for extended periods of time, it is possible to achieve optimal efficacy in chronic conditions where medication must be administered at constant levels, and reduce the side effects [8]. The use of a model drug such as diltiazem hydrochloride (DIL), in combination with magnesium aluminium silicate to achieve controlled drug release, adds value to the importance of using clay minerals as drug carriers [5,6,9].

Peer review under responsibility of Xi'an Jiaotong University.
* Corresponding author.
E-mail address: k.asare-addo@hud.ac.uk (K. Asare-Addo).

https://doi.org/10.1016/j.jpha.2019.12.001

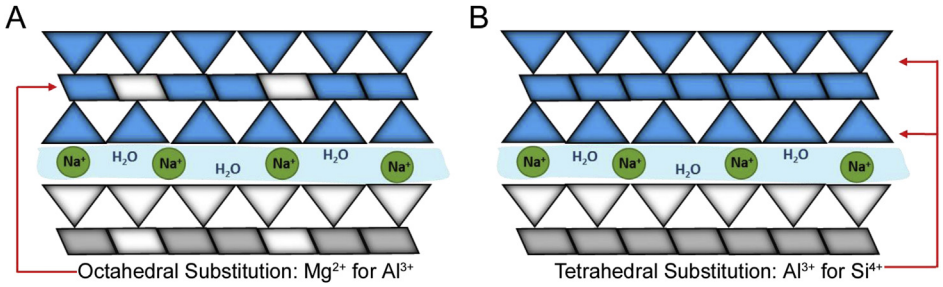

Fig. 1. Montmorillonite (A) and saponite (B) clay structure showing the magnesia or alumina octahedral sheet trapped between two tetrahedral silicate sheets: adapted from [4].

DIL is a non-dihydropyridine calcium channel blocker. It inhibits the calcium channels in the blood vessels, which leads to vasodilatation and, hence, to a lower blood pressure. Furthermore, DIL inhibits calcium channels in the heart, leading to a reduced cardiac contractility and a slower atrioventricular conduction velocity [10,11]. Therefore, DIL represents an efficient treatment for patients suffering from stable chronic angina, due to its ability to reduce myocardial oxygen demand, as it lowers blood pressure, heart rate and cardiac contractility. The drug can also be efficiently used in treating arterial fibrillation due to its ability to control heart rate through its capability to reduce atrioventricular node conduction. DIL's critical drawbacks include an elimination half-life of 3.2 ± 1.3 h following oral administration, and a bioavailability of (42 ± 18)% following first pass metabolism [12]. Therefore, in order to acquire its therapeutic effects and to maintain adequate drug plasma levels, it needs to be administered frequently (3–4 times/day) [13,14]. This model drug therefore represents a suitable target for an extended release formulation. Using clay, instead of the traditionally adopted polymers to control drug release, brings multiple benefits such as overall reduced costs and antibacterial effects, as well as improved kinetics of drug release. This study therefore aims to understand and fully characterise the complexes that are formed between the MAS and DIL that provide the controlled release effect as well as using complex software in understanding the thermodynamics associated with this process.

2. Experimental

2.1. Materials

VEEGUM F EP® (MAS) was a kind gift from R. T. Vanderbilt Company, Norwalk, CT (USA). DIL (MW = 450.98, pKa = 7.8 ± 0.4) was purchased from TCI (Tokyo Chemical Industry), Tokyo. Acetonitrile (HPLC grade) and sodium phosphate, dibasic hydrate, 99+% (HPLC grade), 2 M sodium hydroxide and 2 M hydrochloric acid were purchased from Fisher Scientific, UK.

2.2. Methods

2.2.1. Microscopy studies and formulation of MAS-DIL complex particles

Digital microscopy was used to observe the formation of flocs upon the addition of dilute DIL solution to dilute MAS dispersion (ratio 0.5:1, w/v). The drug to clay ratio used in this study was chosen based on the assay studies presented in Section 3.1. This showed the amount of DIL adsorbed onto the clay was maximum 0.26 g DIL/1 g of MAS. Studies were performed using a VHX2000 Digital Microscope from KEYENCE using a blue daylight filter to enhance the contrast between the flocculated particles and the dispersion media. Pictures were recorded at different mixing time points (2 min, 30 min, 60 min, 120 min, 180 min and 24 h) and were compared. Images of the MAS dispersion prior to DIL addition were also acquired.

For the formulation process, MAS-DIL complex particles were prepared by loading the MAS with DIL twice in order to ensure a high drug adsorption. For the first drug loading, separate DIL solution (2%, w/v) and MAS dispersion (2%, w/v) were prepared under continuous stirring for 24 h at 500 rpm (25 °C). The pH of the prepared MAS dispersion and DIL solution was adjusted to pH 5 using 2 M hydrochloric acid and 2 M sodium hydroxide. After 24 h, the MAS dispersion and DIL solution were combined (1:1, w/w) and the mixture was incubated at 37 °C with shaking for 24 h. Flocculates were observed in the mixture. The MAS-DIL complex dispersions obtained were then filtered using a Buchner filtration apparatus with vacuum. For the second drug loading, previously filtered single drug loaded MAS-DIL complex particles were redispersed into a fresh DIL solution (2%, w/v) and incubated at 37 °C with shaking for 24 h. The MAS-DIL flocculated complexes formed were filtered and dried in the oven at 50 °C for 48 h. The dried double drug loaded MAS-DIL complex particles were ground (10 min) using a Retsch® PM 100 ball mill set at 350 rpm to particle sized at 123–65 μm. The use of the ball mill led to a faster breakdown of the hard particulates to the desired particle size.

2.2.2. Characterisation of MAS-DIL complex dispersions and particles

2.2.2.1. Attenuated total reflectance Fourier transform infrared spectroscopy (ATR-FTIR). ATR-FTIR was used to study the interaction between MAS and DIL at the molecular level. MAS, DIL and MAS-DIL complex particles were analysed from 4000 to 400 cm^{-1} on a Smart Orbit ATR-FTIR machine, using diamond as the ATR crystal.

2.2.2.2. Powder X-ray diffractometry (PXRD). Experiments were performed on a D2 PHASER XRD from BRUKER and sample preparation involved the placement of sample powder onto a transmitter holder and conducted using a similar methodology as reported [15]. Analysis was performed at an angular range 2.5–70° (2θ) and a step angle of 0.02° (2θ) s^{-1}. The X-ray source was generated as a Cu radiation at 30 kV and 10 mA. Experiments were performed in triplicate for reproducibility.

2.2.3. High performance liquid chromatography (HPLC)

An HPLC method was developed and validated for the determination and quantification of both DIL and its main degradant, desacetyldiltiazem (DC-DIL) which was observed in samples. Linearity range, precision, limit of quantitation (LOQ) and limit of detection (LOD) were separately determined for both compounds (DIL and DC-DIL) to validate the method used. The peak area of the standards along with the corresponding drug concentration was used to generate a calibration graph to evaluate linearity (slope,

intercept and coefficient of determination R^2) and determine LOD and LOQ. All experiments were conducted in triplicate. An assay of freshly prepared standard DIL and DC-DIL solutions at four different concentrations (1.00, 10.00, 50.00 and 100.00 μg/mL and 0.83, 8.25, 41.26, 82.52 μg/mL respectively) repeatedly run on the same day or on three different days was used to evaluate the intra- and inter-day precision in terms of standard deviation RSD %.

DIL stock solution and standard solutions in the range 100 to 0.1 μg/mL were prepared in purified water. DC-DIL was formed from DIL via hydrolysis (Fig. 2). DIL stock solution was prepared in dilute acid (2 M HCl) and standard solutions in the range 75 to 0.1 μg/mL were prepared from the stock solution using purified water. Samples were left for 72 h at room temperature until complete hydrolysis occurred (confirmed by HPLC). The concentration of DC-DIL present in the standards was determined from the equilibrated hydrolysis reaction assuming that 100% of the drug hydrolysed was observed, as no traces of the parent drug were observed in solution.

The calibration graphs generated for DIL and DC-DIL were found to be linear over the concentration range studied (1.00, 10.00, 50.00 and 100.00 μg/mL and 0.83, 8.25, 41.26 and 82.52 μg/mL, respectively) ($R^2 \geq 0.9999$ and $R^2 \geq 0.9998$, respectively). Linearity was defined by an equation that was further used in the recovery studies. The method was shown to be precise for the detection of both DIL and DC-DIL, the intermediate and intra-assay precision at four different concentrations on three different days being lower than 2% RSD (Table 1) which complies with the acceptable criteria for quality control of pharmaceutical preparations [16,17]. LOQ (the lowest drug concentration that can be recovered within acceptable limits of precision and accuracy) was found to be 1.72 μg/mL for DIL and 1.65 μg/mL for DC-DIL, indicating the high sensitivity of the proposed method at low concentrations of DIL and DC-DIL. LOD (the lowest detectable amount of drug distinguishable from the blank) was 0.57 μg/mL for DIL and 0.55 μg/mL for DC-DIL, confirming the sensitivity of the method proposed.

2.2.4. Isothermal titration calorimetry (ITC)

ITC was used to investigate the binding between MAS and DIL. Single injections experiment (SIM) and multiple injection experiments (MIM) were performed. The fast titration and versatile SIM experiments were used to initially confirm binding and determine the nature of the interaction, while MIM experiments were used further to characterise the reaction in detail and determine the thermodynamic parameters. Studies were carried out on a Microcal VP ITC micro-calorimeter. The instrument was used in high-gain mode, applying a reference power of 20 μcal s^{-1} whilst stirring the sample cell contents at 307 rpm. The MAS dispersion was added into the sample cell and DIL solution into the syringe for all the experiments.

SIM experiments were performed at three different pH values, i.e., 5, 7 and 9 (25 °C). DIL solution was added in one injection into the sample cell. The SIM experiments were fast titration experiments and the real time binding isotherm observed was analysed using Origin 7.0 (MicroCal, Inc) by comparing the reaction rate at the pH values studied [18].

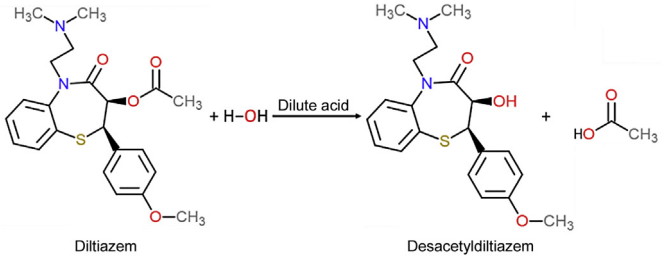

Fig. 2. DIL undergoing dilute acid hydrolysis and product desacetyldiltiazem.

0.010% (w/v) MAS dispersion was prepared under continuous stirring for 24 h, at 25 °C and 200 rpm and was used to fill the sample cell. A 1 mM DIL solution was also prepared separately under stirring for 30 min at 25 °C and 200 rpm prior to the experiments and was independently used to fill the syringe. The drug solution was added as 1 injection of 250 μL into the sample cell containing MAS. The pH of the prepared solutions and dispersions were adjusted using 2 M hydrochloric acid and 2 M sodium hydroxide to 5, 7 and 9. All experiments were conducted in triplicate.

MIM ITC studies were carried out at 25 °C and pH 5, at two different DIL and MAS concentrations. The binding isotherm was studied in 120–140 injections of 2 μL each into the sample cell every 260 s. MAS dispersion (0.036% and 0.010%, w/v) and DIL solution (3.2 mM and 0.45 mM) were prepared. A competitor binding model (Fig. 3) was fitted to the data to get thermodynamic parameters which best reproduce the experimental data using AFFINImeter (AFFINImeter, Spain). The total molar concentration of MAS was estimated and the relative molar fractions of each kind of clay (r_b, r_m) were considered unknown and set as fitted parameter in the analysis.

$$r_b \cdot [B] + r_m \cdot [M] = [MAS]$$

3. Results and discussion

3.1. Observation of floc formation and drug content analysis from MAS-DIL double drug loaded complex particles

The initial analysis of the MAS dispersion using digital microscopy (Fig. 4) allowed the observation of small clay particles dispersed in water forming a colloidal structure, described in literature as the 'house of cards' [4] through the attraction between the negatively charged faces and the partially positive edges of the clay platelets (Fig. 4 A). Following the addition of DIL, the initially monodispersed particles started aggregating as flocs (forming after only 2 min) (Fig. 4 D). With time, flocs were observed to increase in size, became more porous and spread out as the particles clustered together (Figs. 4E–G). After 24 h, a decrease in the size of the flocculated clustered particles was observed as loosely bound aggregates separated away and reattached to other aggregates in a more stable form (Figs. 4H–J) [19]. This process allows the intercalation process to occur after which drug entrapment can be determined.

Determination of drug content in the MAS-DIL double drug loaded complex particles prepared as described in Section 2.2.1 showed discrepancies between the different media used for the dispersion of the complex particles (Table 2). The difference can be related to the behaviour of DIL and MAS in the dissolution media, as well as to the mechanism of adsorption of DIL onto MAS. Results showed that only DC-DIL was recovered by dispersing the MAS-DIL particles in 2 M HCl (Table 2). The degradant was identified following a shift in the retention time on the chromatograms from approx. 7 min (DIL standard solution), to approx. 3.8 min (recovered DIL) (Fig. 5). This behaviour was attributed to the hydrolysis of DIL under acidic conditions and the peak was identified as being DC-DIL, the main degradant of DIL [16,20,21]. A reduction in the exposure time of the MAS-DIL complex to the acid solution from 24 h to 30 min allowed the observation of the two peaks belonging to DIL and DC-DIL on the same chromatogram (Fig. 5B).

Table 1
HPLC method validation for DIL and DC-DIL showing intermediate and intra assay precision at four different concentrations.

Compound	Concentration (μg/mL)	Intermediate precision (RSD, %)	Intra-assay precision (RSD, %)
DIL	1.00	5.32	1.67
	10.00	0.85	0.48
	50.00	0.65	0.17
	100.00	0.55	0.16
DC-DIL	0.83	1.26	0.63
	8.25	0.52	0.91
	41.26	0.25	0.39
	82.52	0.38	0.63

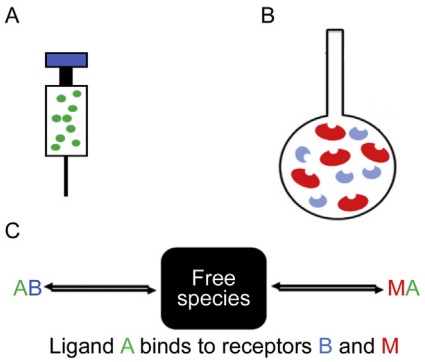

Fig. 3. Competitive ligand binding where A is the ligand in the syringe (DIL) (A), and M and B are the macromolecule and competitive ligand respectively (montmorillonite and saponite making up the MAS), both present in the sample cell (B) and (C) proposes the how ligand A binds to receptors B and M.

Further studies evaluating DIL content in MAS-DIL double drug loaded complex particles by dispersing the particles in ultra-pure water (pH 5) and phosphate buffer (pH 6.8) showed a considerable reduction of DIL degradation. The results showed less than 10% of DIL recovered from the complexes hydrolysed over 24 h in water and phosphate buffer, hence confirming the effect of 2 M HCl on DIL leading to degradant DC-DIL.

Table 2
DIL and DC-DIL content in double drug loaded MAS-DIL complex particles.

Media	Recovered DIL (% w/w)	Recovered DC-DIL (% w/w)
2 M HCl	n/a[$]	25.78 ± 0.32*
Ultra-pure water	16.48 ± 0.42*	1.31 ± 0.03*
pH 6.8 phosphate buffer	17.61 ± 0.22*	1.55 ± 0.02*

Note: [$]DIL completely degraded, hence only degradant DC-DIL recovered.
*values are reported as mg of drug per g MAS.

3.2. Solid state characterisation

3.2.1. ATR-FTIR

ATR-FTIR was used to study the adsorption of DIL onto MAS based on the vibration of chemical bonds formed (Fig. 6). Characteristic peaks were observed on the spectrum of MAS such as the hydroxyl group belonging to Si—OH at 3625 cm^{-1} and the Si—O—Si stretching at 980 cm^{-1}, as well as peaks related to water residues (O—H stretching 3415 cm^{-1}) and water of crystallisation (O—H group bending at 1640 cm^{-1}) [6,7].

The spectrum of MAS-DIL double drug loaded complexes was very different from that of DIL alone, but similar to that of MAS. The presence of the Si—O—Si stretching belonging to the clay was still observed as a broad peak at 980 cm^{-1}. A peak attributed to the hydroxyl stretching of the Si—OH group was observed at 3631 cm^{-1}. The C═O carbonyl groups belonging to DIL at 1680 cm^{-1} and 1740 cm^{-1} and C═C aromatic ring stretching belonging to DIL at

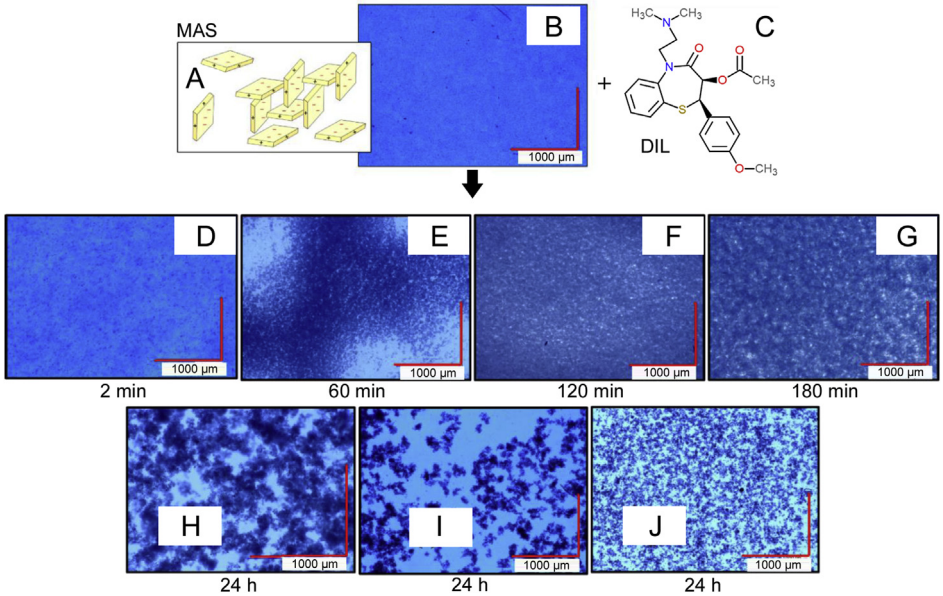

Fig. 4. Scheme of the 'house of cards' formed upon MAS dispersion in water: adapted from Ref. [4] (A); Digital microscopy images of MAS (B); Chemical representation of DIL structure (C); and complexes formed between MAS and DIL at different time points of aggregation (D–J).

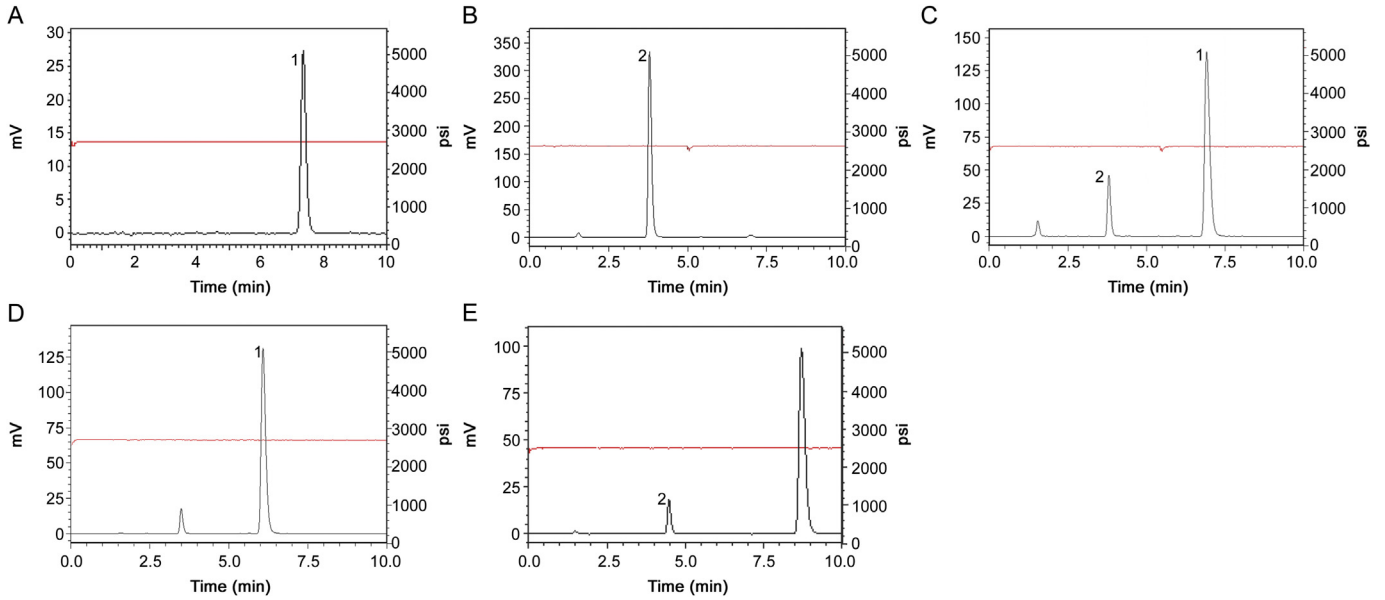

Fig. 5. Typical HPLC chromatograms of DIL standard solution at 25 °C (A) and DIL recovered from MAS-DIL complex using 2 M HCl (24 h exposure) (B), 2 M HCl (30 min exposure) (C), ultra – pure water (D) and pH 6.8 phosphate buffer (E) showing the presence of DIL (1) and degradant desacetyl diltiazem (2).

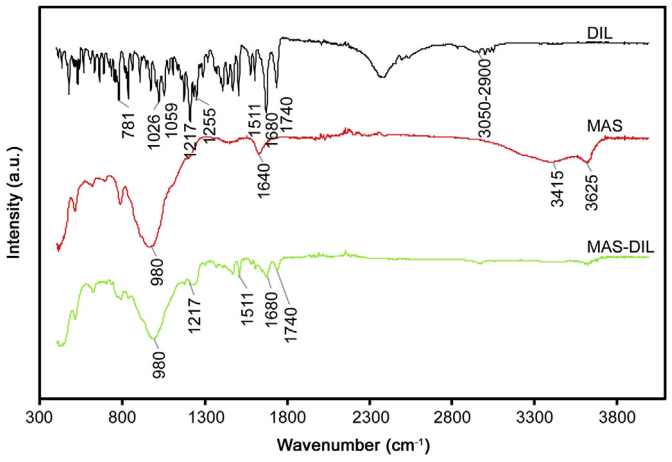

Fig. 6. ATR-FTIR for DIL, MAS and MAS-DIL double drug loaded complex.

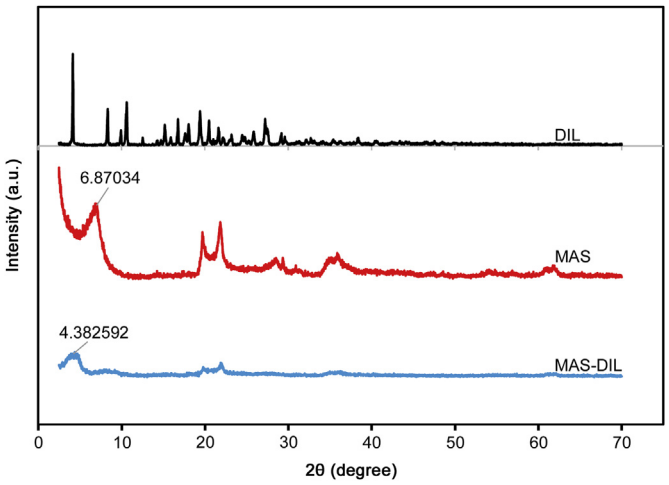

Fig. 7. PXRD patterns of MAS, DIL and MAS-DIL double drug loaded complexes.

1511 cm^{-1} were still observed but all became smaller. The peak belonging to the amine group on the DIL structure observed at 1217 cm^{-1} was still present but became broader. The peaks attributed to R–O–R stretching at 1026 cm^{-1} and C–O ester stretching at 1059 cm^{-1} on DIL structure were not observed on the spectrum of MAS – DIL complex particles. The change and disappearance of some of the peaks characteristic to both DIL and MAS demonstrated the potential interaction between them by the formation of hydrogen bonds between the silanol groups of MAS with the amine and hydroxyl groups of DIL [6,7].

3.2.2. PXRD

The diffractogram acquired for MAS (Fig. 7) displays a distinctive reflection at 6.87034° (2θ) representing the thickness of the basal spacing between the platelets, calculated using Bragg's Law as being 1.28 nm, a value similar to those suggested in the literature [6,9]. The prepared MAS-DIL complex particles were shown to be in amorphous form and did not follow the PXRD pattern of DIL or MAS alone. The amorphous characteristic of the MAS-DIL sample suggests the molecular dispersivity of the drug in the prepared complexes. Furthermore, the reflection at 6.87034° (2θ) on the MAS diffractogram representing the basal spacing was shifted to 4.382592° (2θ) on the MAS-DIL diffractogram and showed a reduced intensity. The peak shift means an increase in basal spacing of MAS from 1.28 nm up to ≈2.016 nm upon intercalation of DIL into the clay platelets, hence confirming the complexation [6,22].

3.3. ITC

3.3.1. Binding between MAS and DIL: single injection experiments

SIM experiments confirmed that binding occurred between MAS and DIL. The binding isotherm between MAS and DIL was shown to be highly exothermic at the pH values studied (Fig. 8). The power signal returned to baseline faster at pH 9 compared with pH 5 and 7, indicating therefore a more rapid interaction. Considering the ionisation of DIL, a more favourable interaction at pH 9 implies that DIL is more readily adsorbed onto MAS via hydrogen bonding

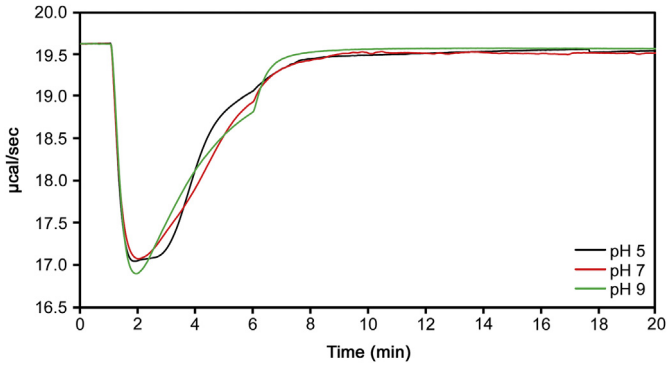

Fig. 8. Titration of DIL solution (pH 5) into MAS dispersion (pH 5) (black), pH 7 (red) and pH 9 (green) at 25 °C.

and water bridging, the drug being mainly present in solution in its unionised form at this pH. This may be explained by the increased length of the alkyl ammonium chain and large molecular weight of DIL, which were shown to result in a greater contribution to adsorption onto the clay via van der Waals forces in previous studies [23,24].

3.3.2. Binding between MAS and DIL: multiple injection experiments

The binding between MAS and DIL was further explored using MIM stepwise experiments at pH 5 and 25 °C. The working pH was chosen based on drug ionisation, DIL being mostly ionised in solution at pH 5 (pK_a 7.8) and hence, expected to interact with the negatively charged faces of MAS platelets [4,25]. Experiments confirmed the binding and showed the presence of more than one binding event at both higher and lower concentrations (Figs. 9 A and B). The experiment at low concentration (Fig. 9 B) allowed the

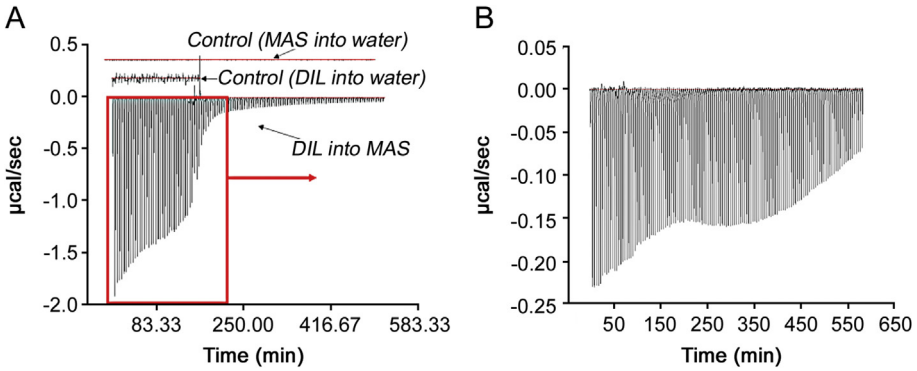

Fig. 9. ITC raw data showing: titration of 3.2 mM DIL into 0.036% MAS and blank titrations (water into MAS 0.036% (w/v) and DIL 3.2 mM into water) (A); titration of 0.45 mM DIL into 0.010% (w/v) MAS (B). All experiments were undertaken at pH 5 and 25 °C.

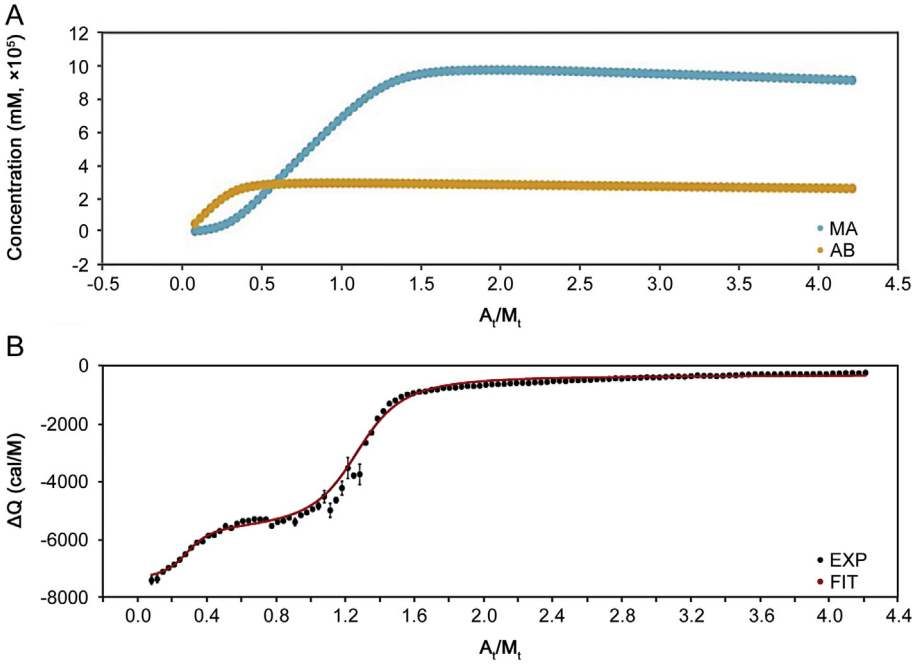

Fig. 10. Species distribution plot showing the binding between ligand A (DIL) and macromolecules M and B (MAS mixture of montmorillonite and saponite) reaching saturation point (A); Thermodynamic profile through a competitive curve fitting model for adsorption of DIL solution (3.2 mM) pH 5 onto MAS dispersion (0.036%, w/v) pH 5 at 25 °C (B).

Table 3
Multiple injection mode calorimetric binding studies studying the adsorption of DIL (3.2 mM) onto MAS (0.036%, w/v) at 25 °C (pH 5). Data analysed through a competitive curve fitting model to calculate affinity (Ka) and changes in enthalpy (ΔH) and entropy (-TΔS).

Reaction	r	Ka (M^{-n})	ΔH (cal/mol)	-TΔS (cal/mol)
M + A ↔ MA	0.76	4.80 E+5 ± 7.59 E+3	−6.71 E+3 ± 1.29 E+1	−9.28E+2
A + B ↔ AB	0.24	2.54 E+7 ± 1.10 E+6	−8.94 E+3 ± 2.18 E+1	−1.02E+3

highly detailed observation of the binding events, confirming that there were no other additional processes taking place. Control binding experiments showed no interaction between MAS dispersion and water, and between DIL solution and water at pH 5 and 25 °C. The presence of multiple binding events following MAS-DIL binding was not observed in the ITC SIM experiments, hence emphasising the importance of MIM stepwise experiments in describing chemical interactions in detail.

A competitor binding model (Fig. 10) was fitted to the data to determine the thermodynamic parameters of the reaction. For this analysis it was assumed that the two different types of clay within MAS (montmorillonite and saponite) placed into the sample cell may potentially interact differently upon the addition of DIL. This assumption was made based on the isomorphic substitution of a limited amount of octahedral Al^{3+} with Mg^{2+} in montmorillonite and the substitution of a limited amount of tetrahedral Si^{4+} by Al^{3+} in saponite, naturally balanced by exchangeable Na^{+} ions that can be easily displaced and replaced, giving the clay the ability to act like a reservoir. Initially the concentrations of both clays were considered equal to total MAS, that is, [B] = [M] = [MAS] and AFFINImeter was used to fit the data with the competitive model using rb and rm (the correction of the nominal concentration of the compounds in the cell) as fitted parameters with the following constraint rb + rm = 1. The fitting of rb and rm allows the calculation of the real concentration of both kinds of clay. The analysis revealed that approximately 24% of the MAS interacts strongly with DIL (K_a = 2.54 E+7 ± 1.10 E+6 M) and 76% of MAS interacts weakly with DIL (K_a = 4.80 E+5 ± 7.59 E+3 M) (Table 3). The binding events had similar negative enthalpies (−6.71 E+3 ± 1.29 E+1 cal/mol and −8.94 E+3 ± 2.18 E+1 cal/mol) and negative entropies −9.28E+2 cal/mol and −1.02E+3 cal/mol (Table 3), suggesting that in both cases the binding was enthalpy driven and entropically unfavourable, as high energy resulted from broken and created hydrogen bonds as well as electrostatic van der Waals interactions. This implies that montmorillonite and saponite are able to adsorb DIL through a similar mechanism due to their similar structure. The presence of the two binding events upon the adsorption of a cationic compound onto MAS has not been reported in the literature before.

4. Conclusions

DIL and MAS complexes which can be used in providing oral controlled release formulation or strategies were successfully made and characterised. The process of binding revealed two binding processes that are being reported for the first time for DIL and MAS. The thermodynamics suggested that the binding processes for these two events were enthalpy driven and entropically unfavourable. The quantification of these complexes also revealed variable behaviour in the various media tested which can inform a formulator decision in appropriate media for testing due to drug degradation in acidic media.

Acknowledgments

The authors acknowledge the University of Huddersfield for funding A.M. Totea. Authors declare that there are no conflicts of interest.

Conflicts of interest

The authors declare that there are no conflicts of interest.

References

[1] M.I. Carretero, M. Pozo, Clay and non-clay minerals in the pharmaceutical industry. Part I. Excipients and medical applications, Appl. Clay Sci. 46 (2009) 73–80.
[2] M.I. Carretero, Clay minerals and their beneficial effects upon human health. A review, Appl. Clay. Sci. 21 (2002) 155–163.
[3] W. Kanjanakawinkul, T. Rades, S. Puttipipatkhachorn, et al., Nicotine-magnesium aluminum silicate microparticle surface modified with chitosan for mucosal delivery, Mater. Sci. Eng. C 33 (2013) 1727–1736.
[4] Vanderbilt Minerals, VEEGUM ® Magnesium aluminum silicate Vanatural® Bentonite clay for personal care and pharmaceuticals. https://www.vanderbiltminerals.com/assets/uploads/documents/technical/VEEGUM_VANATURAL_P_C_Pharma_Web.pdf.
[5] T. Pongjanyakul, S. Rojtanatanya, Use of propranolol-magnesium aluminium silicate antercalated complexes as drug reservoirs in polymeric matrix tablets, Indian J. Pharm. Sci. 74 (2012) 292–301.
[6] S. Rojtanatanya, T. Pongjanyakul, Propranolol-magnesium aluminum silicate complex dispersions and particles: characterization and factors influencing drug release, Int. J. Pharm. 383 (2010) 106–115.
[7] A.M. Totea, I. Dorin, G. Gavrilov, et al., Real time calorimetric characterisation of clay – drug complex dispersions and particles, Int. J. Pharm. X 1 (2019) 100003, https://doi.org/10.1016/j.ijpx.2018.100003.
[8] M.E. Aulton, Aulton's Pharmaceutics, third ed., Churchill Livingstone, Edinburgh, 2007.
[9] T. Pongjanyakul, W. Khunawattanakul, S. Puttipipatkhachorn, Physicochemical characterizations and release studies of nicotine-magnesium aluminum silicate complexes, Appl. Clay Sci. 44 (2009) 242–250.
[10] L. Rodríguez Padial, G. Barón-Esquivias, A. Hernández Madrid, et al., Clinical experience with diltiazem in the treatment of cardiovascular diseases, Cardiol. Ther. 5 (2016) 75–82.
[11] D. Abernethy, J. Schwartz, Calcium-antagonist drugs, N. Engl. J. Med. 341 (1999) 1447–1457.
[12] P. Hermann, S.D. Rodger, G. Remones, et al., Pharmacokinetics of diltiazem after intravenous and oral administration, Eur. J. Clin. Pharmacol. 24 (1983) 349–352.
[13] F. Qazi, M.H. Shoaib, R.I. Yousuf, et al., Formulation development and evaluation of diltiazem HCl sustained release matrix tablets using HPMC K4M and K100M, Pak. J. Pharm. Sci. 26 (2013) 653–663.
[14] J. Li, C. Luo, D. Zhang, et al., Formulation and development of ternary hybrid matrix tablets of diltiazem hydrochloride, Powder Technol. 294 (2016) 66–70.
[15] P.R. Laity, K. Asare-Addo, F. Sweeney, et al., Using small-angle X-ray scattering to investigate the compaction behaviour of a granulated clay, Appl. Clay Sci. 108 (2015) 149–164.
[16] V.A. Chatpalliwar, P.K. Porwal, N. Upmanyu, Validated gradient stability indicating HPLC method for determining diltiazem hydrochloride and related substances in bulk drug and novel tablet formulation, J. Pharm. Anal. 2 (2012) 226–237.
[17] J. Ermer, H.J. Ploss, Validation in pharmaceutical analysis: Part II: central importance of precision to establish acceptance criteria and for verifying and improving the quality of analytical data, J. Pharm. Biomed. Anal. 37 (2005) 859–870.
[18] MicroCal, VP-ITC user's manual, Northampton (1998). https://ctrstbio.org.uic.edu/manuals/vpitc_manual.pdf.
[19] R. Chakrabort, Effects of floc size and shape in particle aggregation, in: G. Droppo, G.G. Leppard, S.N. Liss, T.G. Milligan (Eds.), Flocculation in Natural and Engineered Environmental Systems, CRC Press, Boca Raton, Florida, 2005, pp. 95–120.
[20] F. Sadeghi, L. Navidpour, S. Bayat, et al., Validation and uncertainty estimation of an ecofriendly and stability-indicating HPLC method for determination of diltiazem in pharmaceutical preparations, J. Anal. Methods Chem. (2013), https://doi.org/10.1155/2013/353814. Article ID 353814.
[21] G. Holloway, H. Rowe-Joyce, S. Waha, A stability-indicating HPLC procedure for determination of diltiazem hydrochloride in extemporaneously

compounded oral liquids, Pharm. Technol. Eur. 20 (2008) 38–45, in: http://www.pharmtech.com/stability-indicating-hplc-procedure-determination-diltiazem-hydrochloride-extemporaneously-compounde.
[22] S.S. Ray, P. Maiti, M. Okamoto, et al., New polylactide/layered silicate nanocomposites. 1. Preparation , characterization, and properties, Macromolecules 35 (2002) 3104–3110.
[23] S. Yariv, C. Harold, Organo-Clay Complexes and Interactions, CRC Press, 2001.
[24] B.K.G. Theng, Formation, properties, and practical applications of clay—organic complexes, J. R. Soc. N. Z. 2 (1972) 437–457.
[25] ACD I-Lab. https://ilab.acdlabs.com/iLab2/.